Signal photon flux generated by high-frequency relic gravitational waves*

Xin Li(李昕)[1,2;1)] Sai Wang(王赛)[2;2)] Hao Wen(文豪)[1,2;3)]

[1] Department of Physics, Chongqing University, Chongqing 401331, China
[2] State Key Laboratory Theoretical Physics, Institute of Theoretical Physics, Chinese Academy of Sciences, Beijing 100190, China

Abstract: The power spectrum of primordial tensor perturbations $\mathcal{P}_{\rm t}$ increases rapidly in the high frequency region if the spectral index $n_{\rm t}>0$. It is shown that the amplitude of relic gravitational waves $h_{\rm t}(5\times10^9$ Hz) varies from 10^{-36} to 10^{-25} while $n_{\rm t}$ varies from -6.25×10^{-3} to 0.87. A high frequency gravitational wave detector proposed by F.-Y. Li detects gravitational waves through observing the perturbed photon flux that is generated by interaction between relic gravitational waves and electromagnetic field. It is shown that the perturbative photon flux N_x^1 (5×10^9 Hz) varies from 1.40×10^{-4} s^{-1} to 2.85×10^7 s^{-1} while $n_{\rm t}$ varies from -6.25×10^{-3} to 0.87. Correspondingly, the ratio of the transverse perturbative photon flux N_x^1 to the background photon flux varies from 10^{-28} to 10^{-16}.

Keywords: relic gravitational waves, high frequency gravitational waves detector, signal photon flux

PACS: 04.30.Nk, 98.80.-k **DOI:** 10.1088/1674-1137/40/8/085101

1 Introduction

Gravitational waves (GWs), as a prediction of general relativity, have been detected directly by the LIGO Scientific Collaboration and Virgo Collaboration [1]. It is very interesting and important to search for GWs both in experiments and theories. GW carry away energy. Thus, one of most important theoretical predictions of GWs is that they cause the orbital decay of binary systems. This was first observed in PSR 1913+16 [2]. GWs cause fluctuations of space. Various detectors based on this property of GWs are constructed or proposed to search for GWs in different frequency bands. These include pulsar timing arrays (10^{-9}–10^{-7}Hz) [3], space-based interferometers such as eLISA (10^{-4}–10^{0}Hz) [4], and ground-based interferometers such as LIGO ($10-10^{4}$Hz) [5].

The standard cosmological model, i.e. the ΛCDM model [6, 7] is consistent with several precise astronomical observations made by the Wilkinson Microwave Anisotropy Probe (WMAP) [8], Planck satellite [9], Supernovae Cosmology Project [10] and others. However, the relic gravitational waves (RGWs) that were produced in the inflationary stage [11] of the universe have not been detected. RGWs that could generate B-mode polarizations of cosmic microwave background radiation (CMB) have very low frequency ($10^{-18}-10^{-15}$Hz). The recent joint analysis of BICEP2/Keck Array and Planck Data (BKP) [12] gives severe constraints on B-mode polarizations of the CMB. It gives an upper limit for the tensor-to-scalar ratio $r_{\rm t}$ of $r_{\rm t}<0.12$ at 95% confidence level at the pivot scale 0.01 Mpc^{-1}. The inflation model tells us that RGWs have a broad range spectrum, from 10^{-18} Hz to 10^{10} Hz, where the lower and upper bounds of frequency correspond to the current Hubble radius ($1/H_0$) and the vacuum energy scale during inflation (10^{16} GeV), respectively [13]. Thus, it is expected that GW detectors such as LIGO and eLISA could give information on RGWs. At present, LIGO[14] gives the most severe constraint on energy density of RGWs, i.e., $\Omega_{\rm GW}<5.6\times10^{-6}$ over a frequency band spanning $41.5-1726$ Hz.

The power spectrum of primordial tensor perturbations that is associated with RGWs can be parameterized as [15]

$$\mathcal{P}_{\rm t}(k)=r_{\rm t}A_{\rm s}\left(\frac{k}{k_{\rm p}}\right)^{n_{\rm t}}, \tag{1}$$

where $A_{\rm s}$ is the amplitude of the power spectrum of primordial scalar perturbations, $n_{\rm t}$ is the tensor spectral index and $k_{\rm p}$ is the pivot scale. In the canonical single-field slow-roll inflation models, $n_{\rm t}$ satisfies the consistency relation, i.e., $r_{\rm t}\approx-8n_{\rm t}$ [11]. This means $n_{\rm t}<0$. However, certain inflation models or alternative models,

Received 9 November 2015, Revised 8 March 2016

∗ Supported by National Natural Science Foundation of China (11305181,11322545,11335012) and Open Project Program of State Key Laboratory of Theoretical Physics, Institute of Theoretical Physics, Chinese Academy of Sciences, China (Y5KF181CJ1)

1) E-mail: lixin1981@cqu.edu.cn

2) E-mail: wangsai@itp.ac.cn

3) E-mail: wenhao@cqu.edu.cn

such as inflation with axion potential [16] and the ekpyrotic model [17], predict a blue tensor spectrum, namely, $n_{\rm t}>0$. Thus, the tensor spectral index $n_{\rm t}$ can be used to distinguish different inflation models and alternatives. In Ref. [18], combining the data of BKP and LIGO yields a constraint on $n_{\rm t}$, namely, $n_{\rm t}=-0.76^{+1.37}_{-0.52}$ at the 68% confidence level.

One can find from formula (1) that the power spectrum of primordial tensor perturbations $\mathcal{P}_{\rm t}$ varies rapidly in the high frequency region. Thus, a high frequency GW detector could give a more severe constraint on the tensor spectral index $n_{\rm t}$ if $n_{\rm t}>0$. F.-Y. Li [19] has designed a GW detector that is focused on detection of GWs at high frequency GW spectra (10^9-10^{14} Hz). Recent research on F.-Y. Li's high frequency GW detector can be found in Ref. [20]. In this letter, we will use the data of the Planck satellite [21] to show the amplitude of RGWs in the high frequency region (10^8-10^{10} Hz). Then, we will use the amplitude of RGWs to obtain the expected experimental signals in F.-Y. Li's GW detector.

2 High frequency relic gravitational waves

The energy density of RGWs is given as [22, 23]

$$\Omega_{\rm GW}(k)=\frac{\mathcal{P}_{\rm t}(k)}{12H_0^2}\left(\dot{\mathcal{T}}(\eta_0,k)\right)^2, \tag{2}$$

where $\eta_0=1.41\times10^4$ Mpc is the conformal time at the present epoch, H_0 is the Hubble constant and the dot denotes the derivative with respect to cosmic time t. Here, the $\mathcal{T}(\eta_0,k)$ in formula (2) that represents the tensor transfer function can be approximately described as [22–25]

$$\mathcal{T}=\frac{3j_1(k\eta_0)\Omega_{m0}}{k\eta_0}\sqrt{1+1.36\left(\frac{k}{k_{\rm eq}}\right)+2.50\left(\frac{k}{k_{\rm eq}}\right)^2}, \tag{3}$$

where Ω_{m0} denotes the matter density parameter at the present epoch, $k_{\rm eq}=0.073\Omega_{m0}h^2$ Mpc^{-1} corresponds to the Hubble radius at matter-radiation equality and h denotes the reduced Hubble constant. We can obtain the time derivative of the tensor transfer function from equation (3). It is given as

$$\dot{\mathcal{T}}=\frac{-3j_2(k\eta_0)\Omega_{m0}}{\eta_0}\sqrt{1+1.36\left(\frac{k}{k_{\rm eq}}\right)+2.50\left(\frac{k}{k_{\rm eq}}\right)^2}. \tag{4}$$

By making use of the tensor transfer function (3), we obtain the amplitude of RGWs at present

$$h_{\rm t}(\eta_0,k)=\sqrt{\mathcal{P}_{\rm t}(k)}\mathcal{T}(\eta_0,k). \tag{5}$$

In this paper, to focus on the effect of tensor spectral index $n_{\rm t}$, we fix the value of the tensor-to-scalar ratio $r_{\rm t}=0.05$ to investigate high frequency RGWs. Only the frequency band of RGWs that ranges from 10^8 Hz to 10^{10} Hz is in the detectable region of the high frequency detector [19]. Thus, we investigate the RGWs in this frequency band. In Figs. 1,2, we apply the mean value of cosmological parameters [21] to give the amplitude $h_{\rm t}(\eta_0,\omega_{\rm G})$ and the numerical results of the energy density $\Omega_{\rm GW}(\omega_{\rm G})$, respectively. Here, the frequency $\omega_{\rm G}$ of RGWs and wavenumber k have the following relation $k=2\pi\omega_G$ and the pivot scale is $k_{\rm p}=0.01$ Mpc^{-1}. We choose $n_{\rm t}=-r_{\rm t}/8,0.61,0.87$ to plot Figs. 1,2, corresponding to the consistency relation of the canonical single-field slow-roll inflation models, 68% confidence level bound and 95% confidence level bound, respectively, are constrained by combining the data of BKP and LIGO [18].

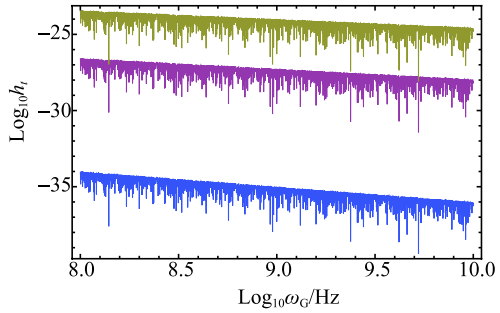

Fig. 1. (color online) The amplitude of relic gravitational waves for various $n_{\rm t}=-r_{\rm t}/8,0.61,0.87$, shown by the blue curve, the purple curve and the brown curve, respectively.

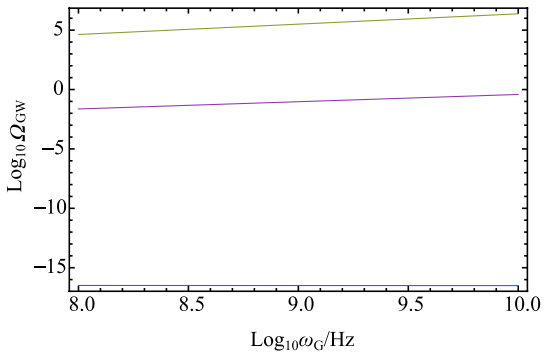

Fig. 2. (color online) The energy density of relic gravitational waves for various $n_{\rm t}=-r_{\rm t}/8$, 0.61, 0.87, shown by the blue curve, the purple curve and the brown curve, respectively.

3 Expected signals in high frequency GW detector

F.-Y. Li's high frequency GW detector [19] applies the electromagnetic perturbation effects produced by high frequency GWs to detect GWs. The designed experimental device is embedded in a cavity. It is constituted by a Gaussian beam (GB) that passes through a static magnetic field. The power of the GB is 10 W, and its frequency mode is given as

$$\psi=\frac{\psi_0\exp(-r^2/W^2)}{\sqrt{1+(z/f)^2}}\exp\left(\mathrm{i}\left((k_\mathrm{e}z-\omega_\mathrm{e}t)-\tan^{-1}\frac{z}{f}+\frac{k_\mathrm{e}r^2}{2R}+\delta\right)\right), \quad (6)$$

where $\psi_0\approx 1.26\times10^3$ Vm^{-1} denotes the amplitude of GB, $f=k_\mathrm{e}W_0^2/2$, $r^2=x^2+y^2$, $W=W_0\sqrt{1+(z/f)^2}$, $W_0=0.05$ m^2 denotes the minimum spot radius and $R=z+f^2/z$ denotes the curvature radius of the wave fronts of the GB at z. The static magnetic field $\bar{B}_y^0$ is designed to be 10 T and pointing along the y-axis. It is localized in the region $-l_1\leqslant z\leqslant l_2$, where $l_1=l_2=0.3$ m. The GB (6) does not have electric field that points along the z-axis. For simplicity, we set background electric field $E_x^0=\psi$ and $E_z^0=0$. Thus, from Maxwell's equation, one can obtain

$$E_y^0=2x\left(\frac{1}{W^2}-\frac{\mathrm{i}k_\mathrm{e}}{2R}\right)\int E_x^0\mathrm{d}y, \quad (7)$$

$$B_z^0=\frac{\mathrm{i}}{\omega_\mathrm{e}}\left(\frac{\partial E_x^0}{\partial y}-\frac{\partial E_y^0}{\partial x}\right). \quad (8)$$

While the high frequency GWs that propagate along the z-axis pass through the cavity, they will produce a perturbed electromagnetic field. If the frequency of GW ω_G equals the frequency of the GB ω_e, the coherence effect magnifies the effect of the GB and produces transverse perturbative photon flux. It has been shown in Ref. [19] that the transverse perturbative photon flux that propagates along the x-axis is larger than the one that propagates along other directions. In this paper, we only focus on investigating the transverse perturbative photon flux that propagates along the x-axis.

The dynamics of the electromagnetic system in the cavity should satisfy the electromagnetic equations in curved spacetime [26], since the spacetime is fluctuated by GWs. These electromagnetic equations can be solved by a perturbation approach, because the amplitude of GWs is very small. By making use of the solutions of these electromagnetic equations, one can obtain the background photon irradiance and the transverse perturbative photon irradiance. The background photon irradiance along the x-axis is given as

$$n_x^0=\frac{1}{\hbar\omega_\mathrm{e}}\left\langle\frac{1}{\mu_0}(E_y^0B_z^0)\right\rangle, \quad (9)$$

where μ_0 is the vacuum permeability. The transverse perturbative photon irradiance along the x-axis is given as

$$n_x^1=\frac{1}{\hbar\omega_\mathrm{e}}\left\langle\frac{1}{\mu_0}(E_y^1B_z^0)\right\rangle, \quad (10)$$

where the perturbed electric field E_y^1 generated from the GW is given as

$$E_y^1=h_\mathrm{t}\bar{B}_y^0c\left(-\frac{1}{2}k_\mathrm{e}(z+l_1)\exp[\mathrm{i}(k_\mathrm{e}z-\omega_\mathrm{e}t)]+\frac{\mathrm{i}}{4}\exp[\mathrm{i}(k_\mathrm{e}z+\omega_\mathrm{e}t)]\right), \quad (11)$$

and c denotes the speed of light. The background photon flux along the x-axis and the transverse perturbative photon flux along the x-axis can be derived from equations (9,10). They are given as

$$N_x^0=\iint_{\Delta s}n_x^0\mathrm{d}y\mathrm{d}z, \quad (12)$$

$$N_x^1=\iint_{\Delta s}n_x^1\mathrm{d}y\mathrm{d}z, \quad (13)$$

where the "typical receiving surface" Δs of the high frequency GW detector equals 3×10^{-2} m^2, i.e., $0<y<0.1$ m, $0<z<0.3$ m.

The transverse perturbative photon flux $N_x^1|_{x=3.5\text{ cm}}$ is shown in Fig. 3. The ratio of the transverse perturbative photon flux N_x^1 to the background photon flux N_x^0, i.e. $S=N_x^1|_{x=3.5\text{ cm}}/N_x^0|_{x=3.5\text{ cm}}$, describes the basic feature of the high frequency GW detector. It is shown in Fig. 4. Figure 4 implies that the spectrum of background

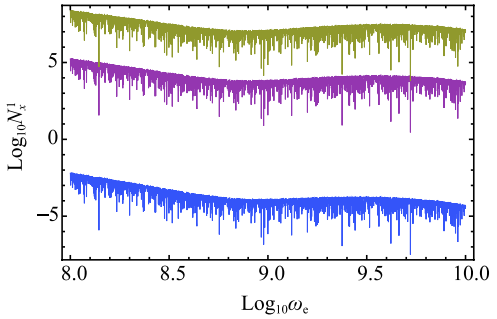

Fig. 3. (color online) The transverse perturbative photon flux $N_x^1(\mathrm{s}^{-1})$ at $x=3.5$ cm for various $n_\mathrm{t}=-r_\mathrm{t}/8, 0.61, 0.87$, shown by the blue curve, the purple curve and the brown curve, respectively.

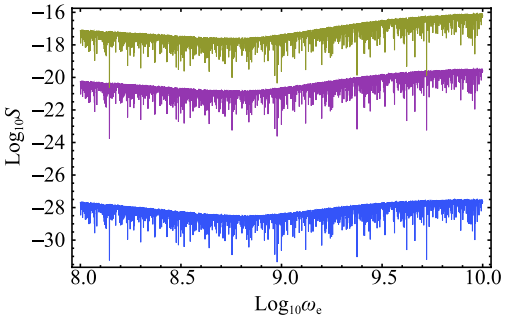

Fig. 4. (color online) The ratio of the transverse perturbative photon flux N_x^1 to the background photon flux N_x^0, i.e. $S=N_x^1|_{x=3.5\text{ cm}}/N_x^0|_{x=3.5\text{ cm}}$, for various $n_\mathrm{t}=-r_\mathrm{t}/8, 0.61, 0.87$, shown by the blue curve, the purple curve and the brown curve, respectively.

photon flux has a different behavior from the spectrum of perturbative photon flux. This means that one can remove the background photon flux from the observed photon flux.

4 Conclusions and remarks

The designed high frequency GW detector, as a new window on the universe, could provide more information on the stage of inflation. The power spectrum of primordial tensor perturbations $\mathcal{P}_{\rm t}$ increases rapidly the in high frequency region if the spectral index $n_{\rm t} > 0$. Thus, a high frequency GW detector could give more severe constraints on the tensor spectral index $n_{\rm t}$. In this paper, we showed the amplitude of RGWs with frequency range of 10^8−10^{10} Hz. It is shown in Fig. 1 that the amplitude of RGWs $h_{\rm t}$ (5×10^9 Hz) varies from 10^{-36} to 10^{-25} while $n_{\rm t}$ varies from $-r_{\rm t}/8$ to 0.87. Interaction between the RGWs and electromagnetic system could generate a perturbed electromagnetic field. F.-Y. Li's high frequency GW detector [19] applies this effect to detect GWs. We have used the designed experimental parameters to calculate the perturbative photon flux N_x^1 that is generated from RGWs. We find from Fig. 3 that the perturbative photon flux N_x^1 decreases while the frequency increases. The scale of the cavity is designed to be 60 cm. These facts imply that F.-Y. Li's detector should focus on detecting RGWs with frequency 5×10^9 Hz such that the wavelength of the RGWs matches the scale of the cavity. The perturbative photon flux $N_x^1|_{x=3.5\ {\rm cm}}(5\times10^9\ {\rm Hz})$ varies from $1.40\times10^{-4}\ {\rm s}^{-1}$ to $2.85\times10^7\ {\rm s}^{-1}$ while $n_{\rm t}$ varies from $-r_{\rm t}/8$ to 0.87. In Fig. 4, we have shown the ratio of the transverse perturbative photon flux N_x^1 to the background photon flux N_x^0, that describes the basic feature of the high frequency GW detector. It varies from 10^{-28} to 10^{-16} while $n_{\rm t}$ varies from $-r_{\rm t}/8$ to 0.87. Our results imply that the spectrum of background photon flux behaves differently from the spectrum of perturbative photon flux. The signal and background photon fluxes also have other different physical behaviors in specific local regions, such as different flux distribution, propagating direction, phase, wave impedance, decay rate, etc. These distinctive behaviors provide a potential way to remove the background photon flux from the observed photon flux.

The noise in a high frequency GW detector is an important consideration in detecting GWs. In order to detect GWs, the ratio of signal to noise should be large enough. For example, thermal noise can be roughly estimated by $k_{\rm B}T$ ($k_{\rm B}$ is Boltzmann constant and T is the temperature of thermal noise). Then, $T < \hbar\omega_{\rm G}/k_{\rm b} \sim 0.24$ K if $\omega_{\rm G} = 5\times10^9$ Hz. However, the noise strongly depends on the experimental setup. Thus, the detailed analysis of the noise in a high frequency GW detector shall be carried out in future work.

We thank Prof. F.-Y. Li for useful discussions.

References

1 B.P.Abbott et al (LIGO Scientific and VIRGO Collaborations), Phys. Rev. Lett., **116**: 061102 (2016)
2 J. H. Taylor and J. M. Weisberg, Astrophys. J., **253**: 908 (1982)
3 G. Hobbs, Class. Quantum Grav., **25**: 114032 (2008); R. Nan et al, Int. J. Mod. Phys. D, **20**: 989 (2011); R. M. Shannon et al, Science, **349**: 1522 (2015); L. Lentati et al (EPTA Collaboration), Mon. Not. Astron. Soc., **453**: 2576 (2015); Z. Arzoumanian et al (NANOGrav Collaboration), arXiv:1508.03024
4 P. Amaro-Seoane et al, Class. Quantum Grav., **29**: 124016 (2012); http://elisa-ngo.org/
5 http://www.ligo.caltech.edu
6 V. Sahni, Class. Quant. Grav., **19**: 3435 (2002)
7 T. Padmanabhan, Phys. Rept., **380**: 235 (2003)
8 E. Komatsu et al (WMAP Collaboration), Astrophys. J. Suppl., **192**: 18 (2011)
9 P.A.R. Ade et al (Planck collaboration), arXiv: 1502.01582; P.A.R. Ade et al (Planck collaboration), arXiv: 1502.01589
10 N. Suzuki et al, Astrophys. J., **746**: 85 (2012)
11 A. Riotto, arXiv:hep-ph/0210162
12 The BICEP2/Keck and Planck Collaborations, Phys. Rev. Lett., **114**: 101301, (2015)
13 H. X. Miao and Y. Zhang, Phys. Rev. D, **75**: 104009 (2007); X.J. Liu, W. Zhao, Y. Zhang, and Z. H. Zhu, Phys. Rev. D, **93**: 024031 (2016)
14 J. Aasi et al (LIGO and Virgo Collaboration), Phys. Rev. Lett., **113**: 231101 (2014)
15 P.A.R. Ade et al (Planck collaboration), arXiv:1502.02114
16 S. Mukohyama, R. Namba, M. Peloso, and G. Shiu, JCAP, **1408**: 036 (2014)
17 J. Khoury, B. A. Ovrut, P. J. Steinhardt, and N. Turok, Phys. Rev. D, **64**: 123522 (2001)
18 Q. G. Huang and S. Wang, JCAP, **1506**: 021 (2015)
19 F. Y. Li, R. M. L. Baker Jr., Z.-Y. Fang, G.V. Stephenson and Z. Y. Chen, Eur. Phys. J. C, **56**: 407 (2008)
20 F.-Y. Li, N. Yang, Z.-Y. Fang, R.M.L. Baker, G.V. Stephenson, and H. Wen, Phys. Rev. D, **80**: 064013 (2009); J. Li, K. Lin, F.-Y. Li, and Y.-H. Zhong, Gen. Relativ. Gravit., **43**: 2209 (2011); H. Wen, F.-Y. Li, and Z.-Y. Fang, Phys. Rev. D, **89**: 104025 (2014); H. Wen, F.-Y. Li, Z.-Y. Fang and A. Beckwith, Eur. Phys. J. C, **74**: 2998 (2014)
21 Planck Collaboration, arXiv:1502.01589
22 M. S. Turner, M. White and J. E. Lidsey, Phys. Rev. D, **48**: 4613 (1993)
23 W. Zhao, Y. Zhang, X. P. You, and Z. H. Zhu, Phys. Rev. D, **87**: 124012 (2013)
24 S. Kuroyanagi, C. Gordon, J. Silk, and N. Sugiyama, Phys. Rev. D, **81**: 083524 (2010)
25 Y. Watanabe and E. Komatsu, Phys. Rev. D, **73**: 123515 (2006)
26 N. D. Birrel and P. C. W. Davies, *Quantum fields in curved space* (Cambridge University Press, New York Melbourne Pp, 1982)